AIAA SciTech Forum
8-12 January 2024, Orlando, FL
AIAA SCITECH 2024 Forum

10.2514/6.2024-0305

Swirl number effect on the unsteady characteristics of turbulent combustion in axial-swirl combustor

Marcel Ilie[1], John Mcafee[2], Valentin Soloiu[3], Mosfequr Rahman[4], Brandon O'Brian[5] and Marcello Gonzalez[6]
Georgia Southern University, Statesboro, GA, 30458

Swirl combustion is one of the most efficient approach to efficient combustion processes and therefore, it has received great interest particularly from aerospace industry. Swirl combustion has been studied in the past both experimentally and computationally. However, in spite of the extended studies, the swirl combustion is still not well understood and therefore, further studies are required. One of the open questions in the swirl combustion is the effect of the swirl number on the combustion efficiency and instabilities. Over decades, extensive experimental and computational studies of swirl combustion have been performed. The experimental studies of swirl combustion are quite challenging due to the unsteady nature of the combustion process. To overcome these challenges, computational studies have been used in the study of turbulent combustion. The present study concerns the effect of the swirl number on the combustion efficiency and flame stability. The combustion efficiency is assessed based on the temperature developed inside the combustion chamber and NOx levels. The effect of air/fuel blowing ratio on the combustion efficiency and instability is also investigated in this research. The computations are carried out using the large-eddy simulation (LES) approach along with the flamelet combustion model. The analysis reveals the unsteady nature of the flame and thus, its departure from the core of the combustor. The analysis also reveals the presence of a region of high level of temperature, NO and CO_2, inside the combustor.

I. Introduction

Swirl combustion is one of the most efficient combustion approaches and it has been used extensively in the aerospace industry. The swirl combustion has proven to enhance the combustion efficiency. However, one of the drawbacks of the swirl combustion is associated with the aeroacoustics and flame instabilities. The flame instabilities can affect the combustion efficiency and performance and thus, a good understanding of the swirling flow on the flame instabilities can improve the combustion efficiency. On the other hand the acoustic instabilities can cause structural damage of the

[1] Assistant Professor, Department of Mechanical Engineering,
[2] Graduate Student, Department of Mechanical Engineering
[3] Professor, Department of Mechanical Engineering
[4] Professor, Department of Mechanical Engineering,
[5] Graduate Student, Department of Mechanical Engineering
[6] Undergraduate Student, Department of Mechanical Engineering

combustion chamber. Therefore, in the past decades significant efforts have been dedicated to the reduction of the acoustic instabilities associated with the combustion processes. However, to be able to achieve an effective control of the acoustic instabilities and to mitigate them it is necessary to have a good understanding of the combustion phenomenon. Usually, the coupling between the unsteady flame, and implicitly heat release, and acoustic pressure oscillations lead to self-excited oscillations which further generate high-level noise and decrease of the combustion efficiency. Usually, the combustion instabilities of swirl combustion are complex phenomena and depend on the interactions among flow fluctuations, acoustic pressure fluctuations and heat release.

Usually, the experimental studies of swirl combustion requires complex and costly equipment and therefore, the computational approaches are a promising alternative to study the swirl combustion. However, the computational studies of the swirl combustion poses significant challenges due to the complex fuel/air interaction, acoustic instabilities, etc. Therefore, the numerical prediction of these complex fluid dynamics requires advanced computational methods.

Over the past decades various computational fluid dynamics (CFD) along with combustion sub-grid scale models have been developed and employed in the study of turbulent combustion. One of the early computational appraohces were based on the Reynolds-averaged Navier-Stokes (RANS) equations. The RANS approach provides a time-averaged solution and thus, it is not suitable for the computation of unsteady, turbulent flows. To overcome the challenges posed by the RANS method, time-dependent computational approaches such as unsteady Reynolds-averaged Navier-Stokes (URANS) were proposed and developed for the numerical prediction of unsteady turbulent flows. It is worth to mention here that the use of unsteady Reynolds-averaged Navier-Stokes (URANS) methods significantly rely on turbulence models to capture all the relevant turbulence scales. Due to the fact that the turbulent combustion is a multi-scale problem, involving a wide range of length and time scales, the use of RANS-based prediction methods remains limited. Although RANS methods are useful for fluid dynamics computations, holding accurately up to some extent, they are usually not suitable or reliable for an accurate prediction of turbulent combustion.

The recent improvements in the processing speed of computers make the applicability of Direct Numerical Simulation (DNS) and Large Eddy Simulation (LES) to turbulent flows more feasible. However, due to a wide range of length and time scales present in turbulent flows, the use of DNS is still limited to low-Reynolds-number flows and relatively simple geometries. It is known that the number of grid points required for DNS is proportional to $Re^{9/4}$. Direct Numerical Simulation of high-Reynolds number flows of practical interest would necessitate high resolution grid requirements that are far beyond the capability of the most powerful computers available now days. In order to overcome the grid requirements issues, turbulence has to be modelled in order to perform simulations for problems of practical interest. Large Eddy Simulation, with a lower computational cost, is a promising alternative method to DNS, for simulations of high Reynolds-number flows. LES methods are capable of simulating flows at high Reynolds number, LES method being independent of Reynolds number. In Large Eddy Simulation, the large scales are directly solved, while the small scales are modelled. Since flow transition is an unsteady process, LES is probably the most affordable computational tool to be used, since it is the only way, other than DNS, to obtain a time-accurate unsteady solution.

II. Computational methods and models

In the present studies, the combustion processes and instabilities in supersonic cavity flow are investigated using LES. Large-eddy simulation is a result of the space-filtering operation applied to the Navier-Stokes equations. The filtered Navier-Stokes equations are:

$$\frac{\partial \overline{u_i}}{\partial x_i} = 0 \tag{1}$$

$$\frac{\partial \bar{u}_i}{\partial t} + \frac{\partial}{\partial x_j}\left(\bar{u}_i \bar{u}_j\right) = -\frac{\partial \bar{p}}{\partial x_i} - \frac{\partial \tau_{ij}}{\partial x_j} + \frac{1}{\mathrm{Re}} \frac{\partial^2 \bar{u}_i}{\partial x_j \partial x_j} \tag{2}$$

where τ_{ij} is the subgrid scale stress (SGS) given by:

$$\tau_{ij} = \overline{u_i u_j} - \bar{u}_i \bar{u}_j \tag{3}$$

and is modeled, where $\overline{u_i}$ is the velocity component of the resolved scales, $\overline{p}$ is the corresponding pressure and Re is the Reynolds number. The filtering procedure provides the governing equations for the resolvable scales of the flow field. Although the continuity equation (1) of the resolved quantities is equal to the original unfiltered one, the filtered momentum equation (2) includes an additional term for the non-resolvable sub-grid scale stresses τ_{ij}, which results from filtering the non-linear convective fluxes. The role of τ_{ij} is to describe the influence of the small–scale structures on the larger eddies.

The Large Eddy Simulation concept leads to a closure problem similar to the one obtained by the Reynolds-averaged approach. Hence it is possible to classify the turbulence models starting with zero-equation models and ending up with Reynolds stress models. The non-resolvable small-scale turbulence in LES is much less problem-dependent than the large–scale turbulence, such that the sub-grid scale turbulence can be represented by relatively simple models such as zero-equation eddy-viscosity models. The Smagorinsky model is an eddy viscosity model based on the Boussinesq approach, assuming that in analogy to the viscous stresses in laminar flows, the turbulent stresses are proportional to the mean velocity gradients or in a general sense to the large scale strain rate tensor $\bar{S}_{ij}$:

$$\tau_{ij} - \frac{1}{3}\delta_{ij}\tau_{kk} = 2\nu_T \bar{S}_{ij} \tag{4}$$

In the present work the SGS proposed by Smagorinsky and Lilly is used. In this analysis the value of Smagorinsky constant was set to 0.1. The SGS stresses are related to the strain rate tensor by SGS viscosity, ν_T:

$$\tau_{ij} - \frac{1}{3}\delta_{ij}\tau_{kk} = 2\nu_T \bar{S}_{ij} \tag{5}$$

The SGS viscosity ν_T is given by:

$$\nu_T = \rho(C_s D_{wall}\Delta)^2 \left|\bar{S}\right| \tag{6}$$

where C_s is the Smagorinsky constant, D_{wall} represents the van Driest wall damping factor, Δ is the filter width and $\left|\bar{S}\right|$ represents the magnitude of the large-scale strain-rate tensor.

$$\bar{S}_{ij} = \frac{1}{2}\left(\frac{\partial \bar{u}_i}{\partial x_j} + \frac{\partial \bar{u}_j}{\partial x_j}\right) \tag{7}$$

$$\left(\bar{S}_{ij}\bar{S}_{ij}\right)^{\frac{1}{2}} = \left|\bar{S}\right| \tag{8}$$

The sub-grid length l is assumed to be proportional to the filter width $\bar{\Delta}$:

$$l = C_s \bar{\Delta} = C_s\left(\Delta_x \Delta_y \Delta_z\right)^{\frac{1}{3}} \tag{9}$$

The filter width $\bar{\Delta}$ is correlated with a typical grid spacing given by the cube root of the cell volume. Taking into account the reduction of the sub-grid length l near solid walls, the length scale is usually multiplied by a Van driest damping function, as

$$l = C_s \bar{\Delta}[1 - \exp(-y^+/25)^3]^{0.5} \tag{10}$$

Although theoretical values of $C_s \approx 0.16$ for homogenous, isotropic turbulence can be found in literature, smaller values are usually applied in LES computations of non-homogenous and non-isotropic flows. All computations in the present work were carried out with a Smagorinsky constant of $C_s = 0.1$, which is a typical value for practical applications of Smagorinsky model.

More complex SGS models have appeared in the literature (for example, the dynamic SGS eddy viscosity models), but they are beyond the scope of the present work.

The 3-D simulations were performed for three different Reynolds numbers, Reynolds number $Re=1.3x10^5$, $Re=2.5x10^5$, $Re=3.8x10^5$. The computational domain is presented in Figure 1. The computational domain and space-discretization are shown in Figure 1. Inlet boundary conditions are assigned to the regions where the air and fuel are injected into the computational domain. An opening boundary condition is assigned to the outlet of the computational domain.

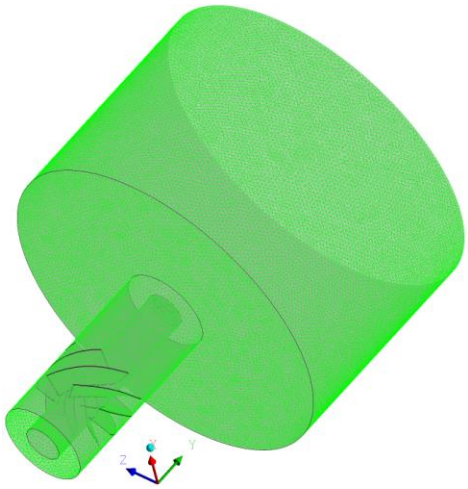

Figure 1. Computational domain-mesh

III. Results and Discussion

Figure 2 presents the time-varying velocity field at different instants in time. The analysis of the velocity field reveals that the flame undergoes significant oscillations and flame breakdowns. The interaction between the flame and freestream flow causes a breakup of the flame and pockets of turbulent eddies are observed inside the combustion chamber. The flame breakdown phenomenon is due to the swirling flow inside the combustion chamber. The high-speed flow entering the combustion chamber breakdown in vortical flow structures which exhibit a wide range of scales and strengths. The swirling flow is also well illustrated by the time-dependent velocity vector field, Figure 3.
The analysis reveals the presence of large vortical structures at the core of the combustion chamber. It is important noting here that the vortical structures oscillate in tandem with the flame and there is a continuous interaction between the vortical structures surrounding the flame and flame itself. The analysis of the velocity field shows that the core of the flow field oscillates the most. The interaction between the swirling flow and core streamflow causes the breakup of the main stream flow. It is expected that these oscillations of the flow field would impact the combustion instabilities and temperatures distribution inside the combustor.

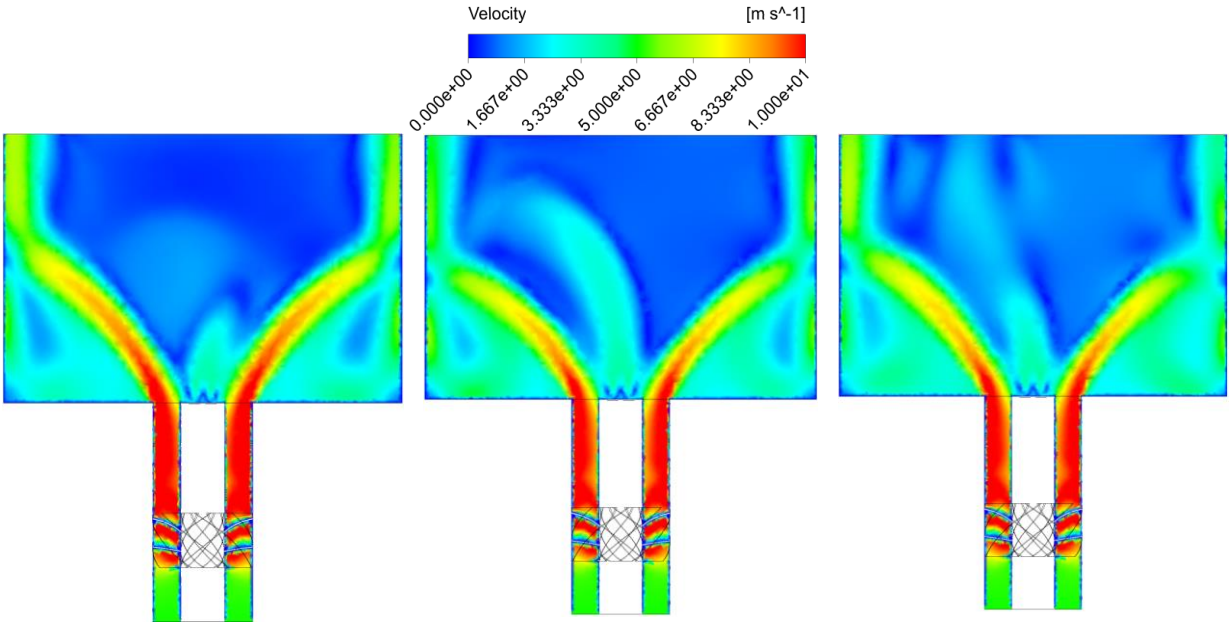

a. t=0.4s b. t=0.5s c. t=0.6s

Figure 2. Time-dependent velocity magnitude

Figure 3 presents the velocity vector field at different instants in time. The analysis of the velocity vector reveals the presence of large recirculation regions inside the combustor chamber. The swirl generates a large magnitude velocity directed towards the walls of the combustion chamber. The interaction between the swirling velocity and core streamflow causes large oscillations of the core streamflow. The swirling flow entrains the core streamflow into a spiraling motion and this is best illustrated by the velocity vector field at different streamwise locations as shown in Figure 5.

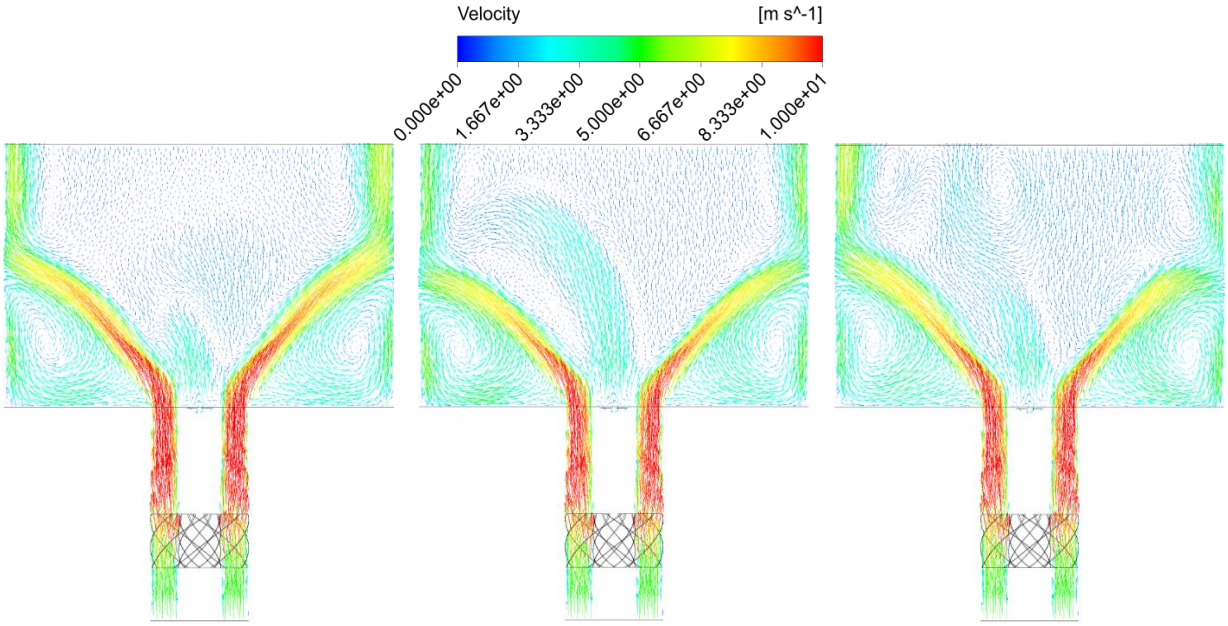

a. t=0.4s b. t=0.5s c. t=0.6s

Figure 3. Time-dependent velocity vector field

Figure 4 presents the time-dependent turbulence kinetic energy (TKE). The analysis of the TKE shows that due to the swirling motion, the flow field exhibits the largest turbulent kinetic energy in the outer regions of the combustion

chamber. The swirl number is the main factor that contributes to the turbulence enhancement and turbulent mixing. The enhancement of the turbulent mixing contributes to the enhancement of the combustion efficiency. Therefore, it is expected that the high temperatures occur in the regions of high turbulence kinetic energy.

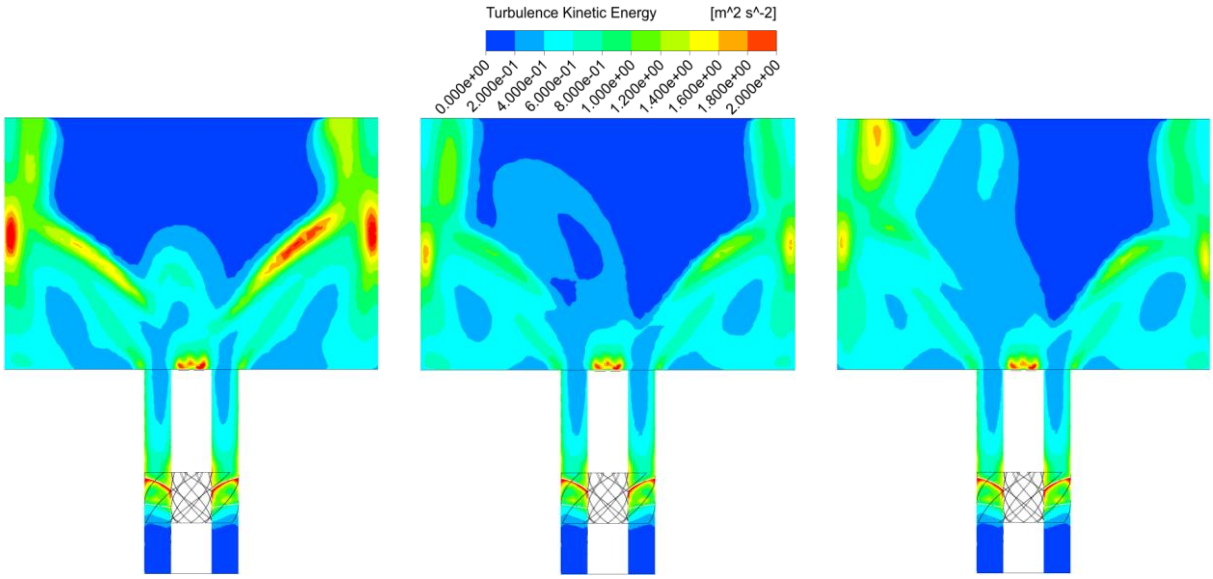

a. t=0.4s b. t=0.5s c. t=0.6s

Figure 4. Time-dependent turbulence kinetic energy

Figure 5 presents the velocity vector field at different streamwise location, inside the combustor chamber. The analysis of the velocity vector field shows the magnitude of the swirling flow which impinges on the walls of the combustor chamber. The swirling flow exhibits the largest magnitude in the region close to the swirl's exit and decays towards the outlet of the combustion chamber. The interaction with core streamflow causes a non-uniform distribution of the velocity vector field. It is expected that this flow field distribution would impact the combustion process in a particular manner.

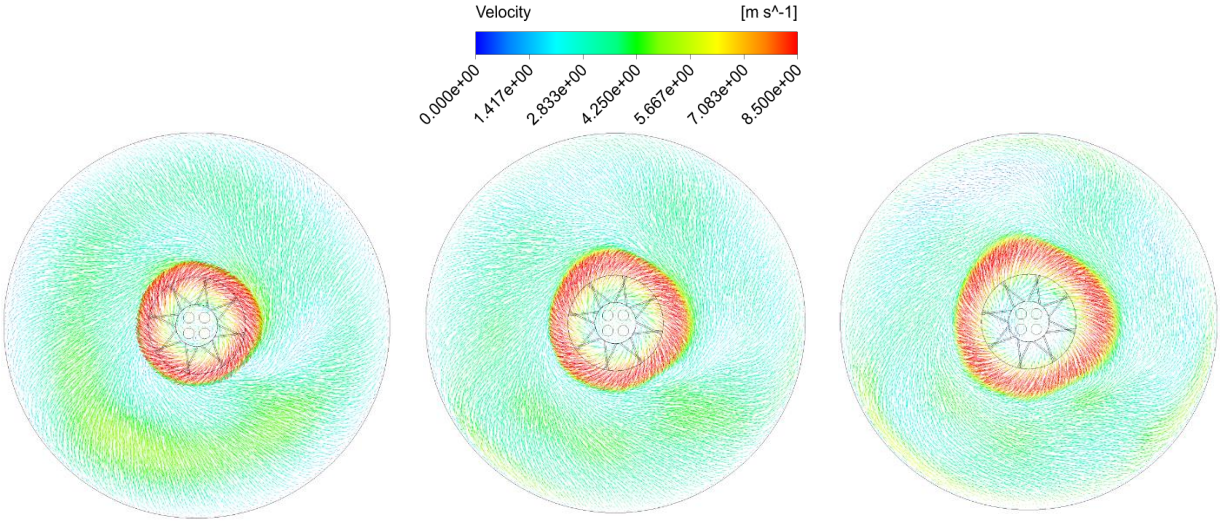

a. y=0.065m b. y=0.07m c. y=0.075m

Figure 5. Time-dependent velocity vector field

Figure 6 presents the turbulence kinetic energy at different streamwise locations. The analysis of the turbulence kinetic energy shows that away from the swirl's exit the size and magnitude of the turbulence kinetic energy regions increase.

These regions are also dominated by the small-scale turbulence eddies as shown in Figure 6. These are also the regions of fast eddy dissipation as shown in Figure 6 which presents the turbulence eddy dissipation.

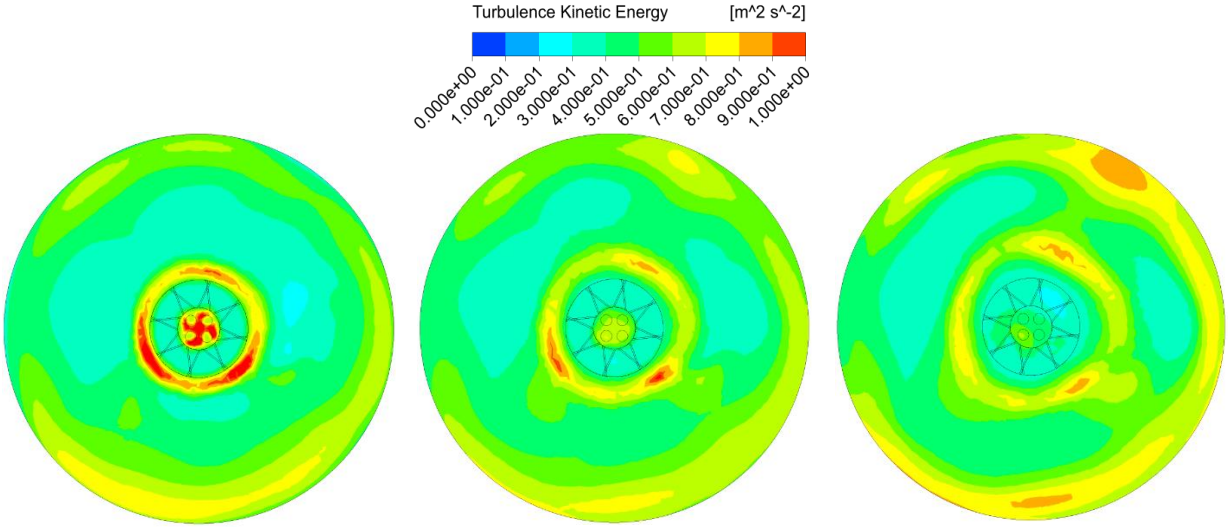

a. y=0.065 b. y=0.07 c. y=0.075

Figure 6. Time-dependent turbulence kinetic energy

Figure 7 presents the time-dependent temperature field at different instants of time. The analysis of the temperature field reveals that the high temperatures occur at the core of the combustion chamber, in the region of high turbulence kinetic energy.

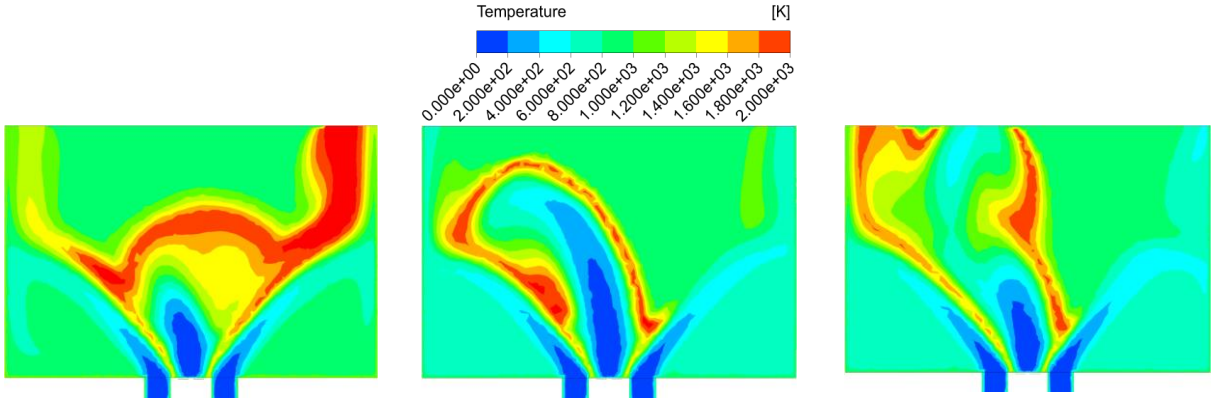

a. t=0.4s b. t=0.5s c.

Figure 7. Time-dependent temperature field

IV. Conclusions

Combustion instabilities of coaxial jet combustor is computationally investigated using the large-eddy simulation (LES) approach. The study reveals that the LES approach captures very well the combustion phenomenon inside the coaxial jet combustor. The analysis reveals that the swirling flow enhances the turbulent mixing and combustion efficiency. The interaction between the swirling flow and core flow causes instabilities of the turbulent flame and therefore, pockets of high turbulence and temperature are observed inside the combustion chamber. The high temperature inside the combustion chamber contributes to the high levels of combustion products. Therefore, the study also reveals that the flow variables velocity, temperature turbulence kinetic energy exhibit oscillatory motion. The analysis reveals the presence of a region of high level of temperature, NO and CO_2, inside the coaxial jet injector.

V. References

[1] K. Jambunathan, E. Lai, M. Moss, B. Button, A review of heat transfer data for single circular jet impingement, International Journal of Heat and Fluid Flow 13 (2) (1992) 106–115

[2] G.M. Carlomagno, A. Ianiro, Thermo-fluid-dynamics of submerged jets impinging at short nozzle-to-plate distance: a review, Experimental Thermal and Fluid Science 58 (2014) 15–35

[3] M. Sabato, A. Fregni, E. Stalio, F. Brusiani, M. Tranchero, T. Baritaud, Numerical study of submerged impinging jets for power electronics cooling, Inter- national Journal of Heat and Mass Transfer 141 (2019) 707–718, doi:10.1016/j. ijheatmasstransfer.2019.06.081.

[4] S. Polat, Heat and mass transfer in impingement drying, Drying Technology 11(6) (1993) 1147–1176

[5] F. Monnoyer, D. Lochegnies, Heat transfer and flow characteristics of the cooling system of an industrial glass tempering unit, Applied Thermal Engineering 28 (17-18) (2008) 2167–2177

[6] A. Sarkar, N. Nitin, M. Karwe, R.P. Singh, Fluid flow and heat transfer in air jet impingement in food processing, Journal of Food Science 69 (4) (2004) CRH113–CRH122

[7] L. Huang, M. El-Genk, Heat transfer and flow visualization experiments of swirling, multi-channel, and conventional impinging jets, International Journal of Heat and Mass Transfer 41 (3) (1998) 583–600

[8] R.C. Chanaud, Observations of oscillatory motion in certain swirling flows, Journal of Fluid Mechanics 21 (1) (1965) 111–127

[9] J. Harvey, Some observations of the vortex breakdown phenomenon, Journal of Fluid Mechanics 14 (4) (1962) 585–592

[10] H. Liang, T. Maxworthy, An experimental investigation of swirling jets, Journal of Fluid Mechanics 525 (2005) 115–159

[11] C. Cala, E. Fernandes, M. Heitor, S. Shtork, Coherent structures in unsteady swirling jet flow, Experiments in Fluids 40 (2) (2006) 267–276

[12] D. Markovich, S. Abdurakipov, L. Chikishev, V. Dulin, K. Hanjalic´, Comparative analysis of low-and high-swirl confined flames and jets by proper orthogonal and dynamic mode decompositions, Physics of Fluids 26 (6) (2014) 065109

[13] A. Ianiro, K.P. Lynch, D. Violato, G. Cardone, F. Scarano, Three-dimensional organization and dynamics of vortices in multichannel swirling jets, Journal of Fluid Mechanics 843 (2018) 180–210

[14] M. Fénot, E. Dorignac, G. Lalizel, Heat transfer and flow structure of a multichannel impinging jet, International Journal of Thermal Sciences 90 (2015) 323–338

[15] G. Vignat, D. Durox, S. Candel, The suitability of different swirl number definitions for describing swirl flows: Accurate, common and (over-) simplified formulations, Progress in Energy and Combustion Science 89 (2022) 100969.

[16] D.H. Lee, S.Y. Won, Y.T. Kim, Y.S. Chung, Turbulent heat transfer from a flat surface to a swirling round impinging jet, International Journal of Heat and Mass Transfer 45 (1) (2002) 223–227

[17] M.-Y. Wen, K.-J. Jang, An impingement cooling on a flat surface by using circular jet with longitudinal swirling strips, International Journal of Heat and Mass Transfer 46 (24) (2003) 4657–4667

[18] H. Yang, T. Kim, T. Lu, K. Ichimiya, Flow structure, wall pressure and heat transfer characteristics of impinging annular jet with/without steady swirling, International Journal of Heat and Mass Transfer 53 (19-20) (2010) 4092–4100

[19] A. Ianiro, G. Cardone, Heat transfer rate and uniformity in multichannel swirling impinging jets, Applied Thermal Engineering 49 (2012) 89–98

[20] K. Nanan, K. Wongcharee, C. Nuntadusit, S. Eiamsa-Ard, Forced convective heat transfer by swirling impinging jets issuing from nozzles equipped with twisted tapes, International Communications in Heat and Mass Transfer 39 (6) (2012) 844–852

[21] Y. Amini, M. Mokhtari, M. Haghshenasfard, M.B. Gerdroodbary, Heat transfer of swirling impinging jets ejected from Nozzles with twisted tapes utilizing CFD technique, Case Studies in Thermal Engineering 6 (2015) 104–115

[22] K. Ichimiya, K. Tsukamoto, Heat transfer from an inflow-type swirling turbulent impinging jet, JSME International Journal Series B Fluids and Thermal Engineering 49 (4) (2006) 995–999

[23] K. Ichimiya, K. Tsukamoto, Heat transfer characteristics of a swirling laminar impinging jet, Journal of Heat Transfer 132 (1) (2010)
[24] Z.U. Ahmed, Y.M. Al-Abdeli, F.G. Guzzomi, Heat transfer characteristics of swirling and non-swirling impinging turbulent jets, International Journal of Heat and Mass Transfer 102 (2016) 991–1003
[25] Z.U. Ahmed, Y.M. Al-Abdeli, F.G. Guzzomi, Flow field and thermal behavior in swirling and non-swirling turbulent impinging jets, International Journal of Thermal Sciences 114 (2017) 241–256
[26] J. Ortega-Casanova, N. Campos, R. Fernandez-Feria, Experimental study on sand bed excavation by impinging swirling jets, Journal of Hydraulic Research 49 (5) (2011) 601–610
[27] J. Ortega-Casanova, CFD and correlations of the heat transfer from a wall at constant temperature to an impinging swirling jet, International Journal of Heat and Mass Transfer 55 (21-22) (2012) 5836–5845
[28] R. Örlü, P.H. Alfredsson, An experimental study of the near-field mixing characteristics of a swirling jet, Flow, Turbulence and Combustion 80 (3) (2008) 323–350
[29] A. Shiri, W.K. George, J.W. Naughton, Experimental study of the far field of incompressible swirling jets, AIAA journal 46 (8) (2008) 2002–2009
[30] G.M. Carlomagno, G. Cardone, Infrared thermography for convective heat transfer measurements, Experiments in Fluids 49 (6) (2010) 1187–1218
[31] J.R. Welty, C.E. Wicks, G. Rorrer, R.E. Wilson, Fundamentals of momentum, heat, and mass transfer, fifth, John Wiley & Sons, 2009.
[32] G. Paolillo, C.S. Greco, G. Cardone, Impingement heat transfer of quadruple synthetic jets, International Journal of Heat and Mass Transfer 135 (2019) 1192–1206
[33] R.J. Moffat, Describing the uncertainties in experimental results, Experimental Thermal Fluid Science 1 (1) (1988) 3–17
[34] R. Goldstein, A. Behbahani, Impingement of a circular jet with and without cross flow, International Journal of Heat and Mass Transfer 25 (9) (1982) 1377–1382
[55] T.S. O'Donovan, D.B. Murray, Jet impingement heat transfer–Part I: Mean and root-mean-square heat transfer and velocity distributions, International journal of heat and mass transfer 50 (17-18) (2007) 3291–3301
[36] Y. Ozmen, E. Baydar, Flow structure and heat transfer characteristics of an un- confined impinging air jet at high jet Reynolds numbers, Heat and mass transfer 44 (11) (2008) 1315–1322
[37] N. Zuckerman, N. Lior, Jet impingement heat transfer: physics, correlations, and numerical modeling, Advances in heat transfer 39 (2006) 565–631